Received 6 May 2023; revised 28 June 2023; accepted 29 June 2023. Date of publication 4 July 2023; date of current version 21 July 2023.
The review of this article was arranged by Editor S. Ikeda.

Digital Object Identifier 10.1109/JEDS.2023.3292298

Scaling Properties of Ru, Rh, and Ir for Future Generation Metallization

MIN-SIK KIM[1], KEUN WOOK SHIN[2], SANG-HOON LEE[1], YONGSUB KIM[1], HYUN-MI KIM[1], SANG-KOOG KIM[1], HYEON-JIN SHIN[2], AND KI-BUM KIM[1] (Member, IEEE)

1 Department of Materials Science and Engineering, Seoul National University, Seoul 08826, South Korea
2 Samsung Advanced Institute of Technology, Samsung Electronics, Suwon 16678, South Korea

CORRESPONDING AUTHORS: K.-B. KIM AND H.-J. SHIN (e-mail: kibum@snu.ac.kr; hyeonjin.shin@samsung.com)

(Min-Sik Kim and Keun Wook Shin contributed equally to this work.)

ABSTRACT The downscaling of metal lines in CMOS devices to subnanometer sizes leads to an increase in their resistivity. Thus, the lower electron mean free paths of Ru, Rh, and Ir make them promising materials to replace Cu in conventional interconnected structures with sub-ten-nanometer dimensions. In this study, we investigate their scaling effects on the resistivities of metal lines with thicknesses of 4–32 nm. The resistivities of Ru, Rh, and Ir as-deposited films prepared via sputtering are lower than that of a Cu film with a sub-ten-nanometer thickness. Despite their similar electron mean free paths, the difference in their bulk resistivities lead to Ir and Rh having lower resistivities than Ru, even after annealing at 400 °C. Their resistivities before and after annealing were fitted with equations based on the Fuch–Sondheimer and Mayadas–Shatzkes models, which assess the contributions of surface and grain boundary scatterings, respectively. We determined that grain boundary scatterings have a significant effect on the resistivities of Ru, Ir, and Rh, whereas surface scatterings have a minimal effect. In addition, in the case of Ru, the effect of the surface roughness on the resistivity was also investigated by measuring the resistivity of Ru films deposited by atomic layer deposition. A high surface RMS roughness of 1–2 nm causes a significant increase in the resistivity at thicknesses below 10 nm that cannot be explained by the aforementioned models. These results present multiple points for consideration when applying short mean free path metals to finite size interconnects.

INDEX TERMS Back-end-of-line, interconnect, Ir, Rh, Ru.

I. INTRODUCTION

Semiconductor processes have advanced to make chips faster and more inexpensive by reducing the pitch size of integrated circuits. As a result, the dimensions of interconnect metals in back-end-of-line (BEOL) have decreased. Cu has been used as a standard main metal in interconnect structures. However, two major problems have emerged because of the decreasing dimensions of Cu interconnects. The reliability, which is related to the electro-migration or formation of stress, induced voids at increased operating current densities and temperatures [1], [2]. As such failures occur by thermally activated atomic diffusion, replacing Cu with metals with a higher melting point can be advantageous. Another problem is the increase in the resistance-capacitance (RC) delay with increasing Cu resistivity, which limits the performance of the integrated circuit [3], [4]. The bulk resistivity (ρ_0) of Cu, which is mainly dominated by phonon scattering, is relatively low, 1.6 $\mu\Omega$-cm. However, its resistivity significantly increases as the dimension of the Cu line decreases to several tens of nanometers [5]. This increase in resistivity is related to electron scatterings at surfaces and grain boundaries [6].

The most common classical models, which describe both electron scattering modes in metals, were proposed by Fuch–Sondheimer (FS) and Mayadas–Shatzkes (MS) [7], [8], [9], [10]. When the thickness and grain size of any metal is less than an electron mean free path (λ), the electrons experience scattering at its surface and grain boundaries before traveling λ, which increases its resistivity, respectively. Hence, in

the case of Cu, where the λ is 40 nm, additional scatterings occur in small dimensions less than 40 nm. Moreover, diffusion barriers, such as TaN and TiN, should be used to ensure the reliability of Cu-based interconnects [11], [12]. However, their higher resistivities compared to Cu reduce the effective dimension of Cu in interconnect structures. These factors increase the resistivity of Cu, rendering Cu difficult to adapt in interconnect structures downscaled to a sub-ten-nanometer scale. As the λ, ρ_0, and melting point are intrinsic characteristics of a material, alternative metals are needed to overcome these limitations of Cu and address the long-term downscaling problems of conventional interconnect structures.

Both the FS and MS models are expressed as a function of λ and ρ_0. They imply that a metal with a short λ and low ρ_0 can maintain a low resistivity in small dimensions. Thus, $(\rho_0 \times \lambda)^{-1}$ is a useful starting point that can be considered as a figure of merit (FoM) when searching for promising candidates for future interconnects [6], [13].

Among them, Co and Ru, which are used as liners in Cu interconnects, have attracted attention as next fill metals in interconnect structures with thinner liners or diffusion barriers compared to those of Cu [14], [15], [16], [17], [18]. In particular, platinum-group metals, including Ru, are more advantageous than Co in terms of their resistivity because of their higher FoMs. Dutta et al. compared the resistivities of Ru, Pd, Ir, and Pt layers in the thickness range 3–32 nm [13]. They showed that Ru and Ir had lower resistivities than Pt and Pd with higher FoM values. In addition to Ru and Ir, Rh also has a high FoM, which is similar to that of Ir. Ru, Ir, and Rh are promising metals that could potentially replace conventional Cu in downscaled BEOL structures. Whereas the deposition of Ir thin films and have recently been reported [19], [20], [21], experimental studies of Rh have been barely conducted.

In addition, considering the practical BEOL process, atomic layer deposition (ALD) of such materials is an effective technique that shows outstanding conformality and thickness controllability. Ru has been developed with various precursors through ALD [22], [23], [24], [25]. However, the surface might be roughened at the initial deposition stage depending on ALD conditions such as precursors and substrates. Therefore, the high surface roughness of Ru by ALD is an issue that limits its dimension as it can affect the surface scattering of electrons. Thus, such effects on the resistivity should also be considered.

In this study, we systematically investigated the scaling effects of Ru, Rh, and Ir in terms of their resistivities with annealing as future interconnect metals. Ru, Rh and Ir films were deposited in the thickness range of 4–32 nm by sputtering and their resistivities were compared before and after annealing. Grain size effects were also studied by replotting the resistivity as a function of the measured grain sizes. Through this, the annealing effects on the resistivities of Ru, Rh, and Ir were confirmed, and we modeled their resistivities by applying FS and MS approaches. From these models, we systematically clarified the major scattering mechanism of each metal in scaled dimensions under the same annealing condition [13], [42]. Finally, we investigated the effect of the surface roughness on the resistivity by analyzing Ru films deposited by ALD at the early stage.

II. EXPERIMENTAL DETAILS

A. METAL FILM DEPOSITION BY DC MAGNETRON SPUTTERING

All Ru, Rh, and Ir films were deposited on 100 nm-thick SiO_2 on Si(001) templates (3 cm × 3 cm in size) at room temperature using a home-made DC magnetron sputtering machine. After loading samples into the chamber, it was pumped down to 3×10^{-8} Torr. Subsequently, Ar flowed at 8 sccm until the chamber pressure reached 1 mTorr. The depositions of the metal films were conducted at a DC power of 50 W. During the deposition process, the target-to-substrate distance was maintained at 40 cm and the deposition rates of Rh, Ir, and Ru were 0.3, 0.2, and 0.2 nm/s, respectively. The thicknesses of the metals were varied in the range 4–32 nm by varying the deposition time. The metal films were annealed at 400 °C in a furnace chamber. Annealing was performed in an Ar ambient for 30 min and the working pressure was maintained at 20 mTorr.

B. ATOMIC LAYER DEPOSITION OF RU FILMS

Ru films were deposited on 100 nm-thick SiO_2 on Si templates at 220 °C in a traveling wave-type ALD apparatus using [(η6-1-isopropyl-4-methylbenzene)(η-4cyclohexa-1,3-diene)ruthenium, DNF Co.] as a precursor for Ru. The precursor was bubbled at 70 °C and carried to the process chamber by 200 sccm of Ar (99.999%). To prevent the condensation of the precursor, the delivering precursor line was maintained at 70 °C. Diluted O_2 was used as a reactant. Each ALD cycle consisted of a Ru precursor pulsing for 10 s, Ar purging for 5 s, diluted O_2 pulsing for 2 s, and Ar purging for 5 s. The flow rate of purging was 200 sccm.

C. FILM CHARACTERIZATION

To calculate the resistivities of the films, the sheet resistances and film thicknesses were measured by four-point probe systems (QuadPro, Signatone) and X-ray reflectivity (XRR, X'pert Pro, PANalytical) using the Cu Kα1 radiation, respectively. The micro-structure and grain size of the metal films were analyzed by high resolution transmittance electron microscopy (TEM, JEM-3000F, JEOL) and X-ray diffractometry (D8-advanced, Bruker) using Cu Kα1 radiation. The TEM samples were prepared by depositing both metals on TEM grids that contained 15 nm-thick Si_3N_4 membranes. Even though we changed template from SiO_2 to Si_3N_4, the average grain sizes of metals were barely changed. Atomic force microscopy images of the metal surface roughness were obtained using an NX-10 system (Park Systems).

III. RESISTIVITY MODELING

The classical resistivity models of MS (grain boundary scattering) and FS (surface scattering) were applied to interpret the experimental results. The models describe an increase in the resistivity with a decrease in characteristic length scales (grain size g and thickness d) owing to increased scattering at the surface and grain boundary by scaling [7], [8], [9], [10]. The resistivity of metals depending on size can be expressed by applying Matthiessen's rule as shown in (1).

$$\rho_{total} = \rho_0 + \Delta\rho_{MS} + \Delta\rho_{FS}\left(1 + \frac{r_1}{n_{RK}}\right) \quad (1)$$

In (1), the increased resistivity by the grain boundary scattering ($\Delta\rho_{MS}$) in the MS model is given by (2):

$$\Delta\rho_{MS} = \rho_{MS} - \rho_o = \frac{\rho_o}{3}\left[\frac{1}{3} - \frac{1}{2}\alpha + \alpha^2 - \alpha^3 ln\left(1 + \frac{1}{\alpha}\right)\right]^{-1} - \rho_o \quad (2)$$

where α is $(\lambda/g)R/(1–R)$ and R is the probability of reflection at the grain boundary, which is allowed to take values between 0 and 1. $R = 0$ corresponds to an electron being fully transmitted through the grain boundary without any loss of momentum in the direction of the electric field. Thus, grain boundary scattering contributes to the resistivity. $R = 1$ refers to an electron being fully reflected from the grain boundary, leading to an infinite resistivity.

Conversely, according to the FS model [8], as shown in (3), the resistivity changes by surface scattering ($\Delta\rho_{FS}$).

$$\Delta\rho_{FS} = \rho_{FS} - \rho_o = \rho_o\left[1 - \frac{3}{2k}(1-\mathbf{p})\int_1^\infty \left(\frac{1}{t^3} - \frac{1}{t^5}\right)\frac{1 - e^{-kt}}{1 - \mathbf{p}e^{-kt}}dt\right]^{-1} - \rho_o \quad (3)$$

In (3), κ is d/λ and t = 1/cosθ, where θ is the scattering angle of the electrons. For a forward moving electron, θ varies between 0° and 90°. Thus, the lower and upper limits of t are 1 and ∞, respectively. p is the specular scattering coefficient, which is the probability that an electron will be specularly reflected upon scattering from a film surface and takes on values in the range 0–1. $p = 1$ corresponds to specular scattering, where the electron conserves the momentum in the direction of its motion after scattering. $p = 0$ is a condition for diffusive scattering, where the electron loses its momentum in the direction of motion after being scattered. Several studies indicated that the variation of p is originated from the created local potential at the surface by adsorption of the atomic or molecular species [26], [27], [28], [29], [30].

IV. RESULTS AND DISCUSSIONS

The resistivities of Ru, Rh, and Ir films with various thicknesses deposited by sputtering were measured to investigate the effect of the λ on the resistivity. Fig. 1 shows the thickness dependences of the resistivities of as-deposited Ru, Rh, and Ir with λ values of 6.6, 6.9, and 7.1 nm, respectively. For comparison, we inserted previously reported data of Cu, which has a relatively longer λ of 40 nm compared

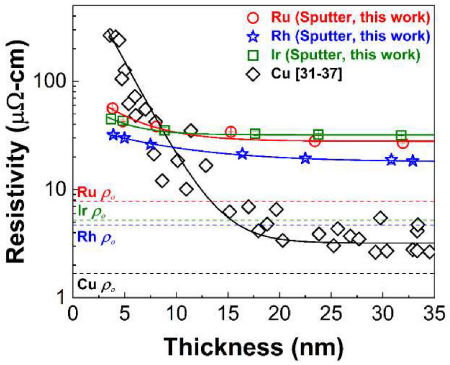

FIGURE 1. Plot of resistivities of as-deposited Ru, Rh, and Ir depending on their thicknesses. Previously reported Cu results are plotted together for comparison [31], [32], [33], [34], [35], [36], [37].

to those of Ru, Rh, and Ir. All reference Cu films were prepared by physical vapor deposition (i.e., sputtering, evaporation, and ion beam deposition) [31], [32], [33], [34], [35], [36], [37]. Among the four metals, Cu has the lowest resistivity of approximately 3.2 μΩ-cm at 30 nm. However, it increases considerably by 70 times (230 μΩ-cm) when the thickness decreases to 4 nm. This increase is ascribed to the combination of the increased surface and grain boundary scatterings at thicknesses less than the λ. In the same thickness range of 4–32 nm, resistivity changes of Ru, Rh, and Ir show much weaker thickness dependences compared to Cu. The resistivities of Ru, Rh, and Ir increase from 26.9, 18.8, and 31.4 μΩ-cm to 56.2, 31.9, and 44.8 μΩ-cm, respectively, when their thickness is decreased from 32 to 4 nm. In three metals thinner than 10 nm, the resistivity of Rh remains lower than that of Ru and Ir, which might be due to its low ρ_0 of 4.7 μΩ-cm (7.8 μΩ-cm for Ru and 5.2 μΩ-cm for Ir) and crossover with that of Cu at a thickness of 9.6 nm (8.9 nm for Ir and 8.6 nm for Ru). In terms of resistivity, this result clearly shows the advantages of metals with short λ values in the sub-nanometer scale and Rh seems to be the most advantageous of the three metals.

To determine the origin of the resistivities of all three metals, we considered both scattering modes, namely surface and grain boundary scattering. While the resistivity owing to the surface scattering is only related to the film thickness according to (3) from the FS model, (2) from the MS model explains that the grain boundary scattering is dependent on the grain size. Thus, we analyzed the crystal structures and grain sizes of each metal using plan-view TEM. To study the grain size effects on the resistivity further, we annealed three metals at the thickness range of 4–32 nm at 400 °C for 30 min. Fig. 2(a) includes bright field (BF) TEM images of as-deposited and annealed Ru, Rh and Ir films with 8 nm-thicknesses. The TEM images clearly show that poly-crystalline metal films were deposited. After annealing at 400 °C, the grains of Ru and Rh are enlarged but Ir appears unchanged. From the BF-TEM images, we

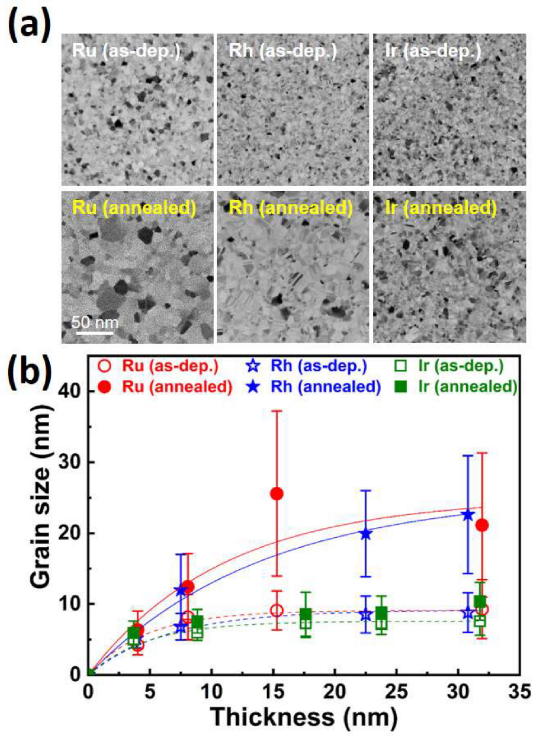

FIGURE 2. **(a) Plan-view transmittance electron microscopy images of as-deposited and annealed Ru, Rh, and Ir films with thicknesses of 8 nm. (b) Grain size distributions of Rh, Ru, and Ir for both as-deposited and annealed films as a function of the film thicknesses.**

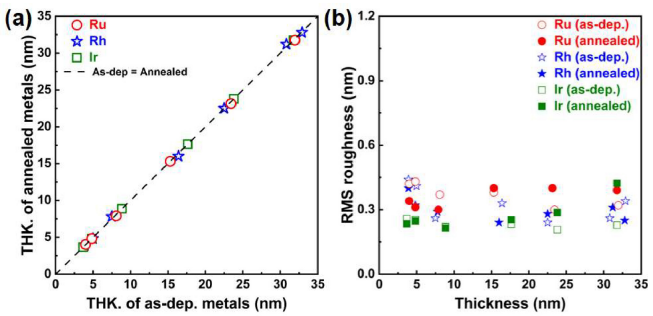

FIGURE 3. **Changes of (a) thicknesses and (b) RMS roughnesses of Ru, Rh, and Ir films after annealing at 400 °C.**

measured the grain sizes of as-deposited and annealed metal films and plotted them as a function of the thickness, as shown in Fig. 2(b). The grain sizes of as-deposited Ru, Rh, and Ir increased to 9.1, 8.9, and 7.5 nm, respectively, as their thicknesses increased up to 15 nm and became saturated when the thicknesses were increased further. For Ru and Rh, grains are almost doubled at the same thickness by annealing at 400 °C. Their variations are also increased because of abnormal grain growth, as shown in Fig. 2(a). However, the grain size of Ir increased 20–30% even after inducing heat budgeting similar to Ru and Rh. These difference between Ir and the other two metals might be due to the high diffusion energy of Ir [38].

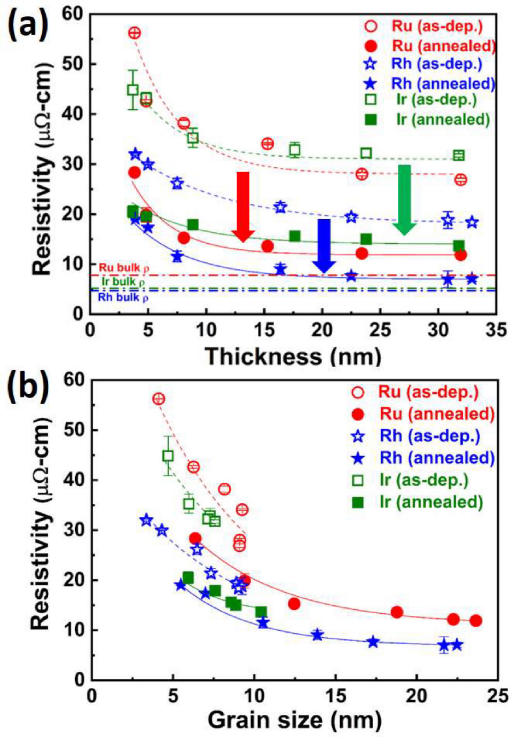

FIGURE 4. **(a) Thickness dependence of the thin film resistivity of both as-deposited and annealed metals. (b) Grain size dependence of the thin film resistivity of both as-deposited and annealed metals.**

Unlike their grain sizes, the surface roughnesses and thicknesses of the three metal films did not change significantly during annealing as shown in Fig. 3.

Fig. 4(a) shows the resistivities of as-deposited and annealed Ru, Rh, and Ir depending on their thicknesses. The resistivities of the three metals are lowered after annealing. Therefore, we conclude that this resistivity lowering is mainly due to the reduction in the electron scattering at the grain boundaries by the enlarged grains when excluding other factors such as surface roughness and thickness changes by annealing. For further investigation of the grain size effects on the resistivities, we replotted the resistivities of Ru, Rh, and Ru as a function of their grain sizes, as shown in Fig. 4(b). When the as-deposited metals have similar grain sizes, their resistivities are in the order of Ru, Ir, and Rh, following the order of their bulk resistivities. Furthermore, it is clearly shown that the resistivities have a strong dependence on the grain size. This trend is maintained after annealing. In addition, it is confirmed that Ir films thicker than 7 nm shows higher resistivities than those of Ru due to the relatively small change in grain size by annealing. However, even at the same grain size, annealed metals have lower resistivities than those of as-deposited ones. During recrystallization by annealing, the average misorientation angle between grains is reduced owing to the preferred movement of large-angle grain boundaries that reduce the reflection probability at the grain boundaries [39]. In the case of Cu, the resistance of

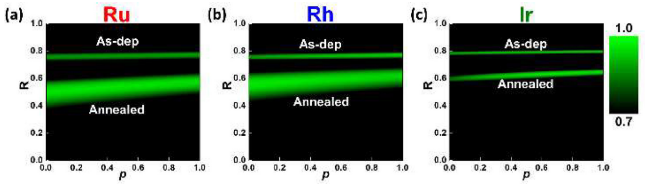

FIGURE 5. Determination coefficient (R^2) of fits to the experimental data, where R and p are fitting parameters for as-deposited and annealed (a) Ru, (b) Rh, and (c) Ir.

the boundaries between randomly oriented grains is reported to be much larger than that of coincidence grain boundaries [40], [41], [42]. We believe that similar phenomena occurred for Ru, Rh, and Ir. From the aforementioned results, we note that the resistivities of Ru, Rh, and Ir are further reduced by decreasing the reflection probability at the grain boundaries and increasing the grain size by annealing.

In addition to grain boundary scattering, the surface scattering also affects the resistivity of a metal. To investigate the effects of surface electron scatterings on the resistivities of Ru, Rh, and Ir, we fitted them based on the FS and MS models using (1), (2), and (3). Fig. 5 shows the mapping images of the determination coefficient (R^2) of different fits, which indicate the sum of square roots of errors between the measured and calculated results as a function of the fitting parameters p and R for the as-deposited and annealed metals. If the calculated values are perfectly matched with the measured ones, then $R^2 = 1$, while the increased error decreases the R^2. As shown in Fig. 5(a), the R of as-deposited and annealed Ru are well defined in a specific range. As mentioned earlier, a reduction of the average misorientation of adjacent grains during the recrystallization process clearly reduces the reflection probability of R from 0.74 to 0.5. In addition, the best fitting range of R (width along the y-axis) becomes six times wider after annealing, which indicates that the resistivity of a metal with large grains is insensitive to the change in the grain boundary properties, such as R. Conversely, because of the small contribution of surface scatterings, the maximum of the R^2 formed continuous lines for p = 0–1. As-deposited and annealed Rh films exhibit a similar trend as Ru, as shown in Fig. 5(b). However, Ir has a slightly different trend, as shown in Fig. 5(c). As the grain size of Ir does not significantly increase after annealing, the best fitting range width of R is maintained at a similar level but the R value is significantly decreased from 0.77 to 0.6. This indicates that the misorientation between grain boundaries decreases after annealing. The maximum of R^2 also formed continuous lines for p = 0–1. From the above mappings that all three metals form a continuous line along the p from 0 to 1, we determined that the resistivity of Ru, Rh, and Ir is mainly influenced by grain boundary scatterings rather than surface scatterings. Indeed, Ezzat et al. investigated the resistivity change of a single crystal Ru by modifying the surface

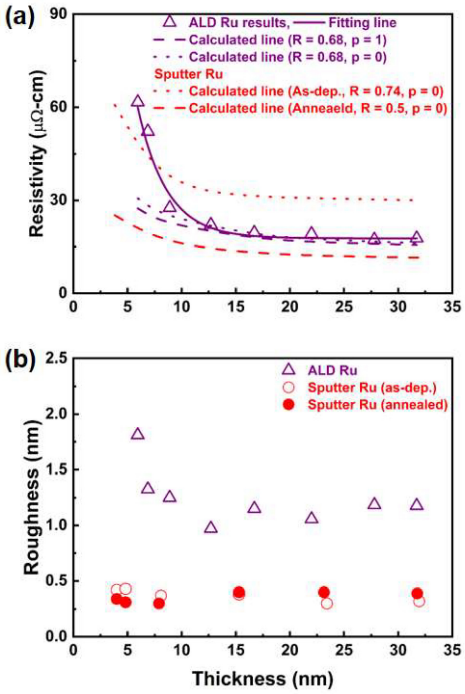

FIGURE 6. (a) Resistivity of atomic layer deposited (ALD) Ru as a function of thickness. The calculated resistivity lines are plotted together for comparison. (b) Surface RMS roughness of ALD, as-deposited, and annealed sputter Ru.

properties [43]. They reported that the resistivity variation was less than 0.5 $\mu\Omega$-cm, which is only 5% of the total resistivity at a thickness of 20 nm, even if p was nearly fully changed from 0 to 1. In our case, specifically defining p is difficult because additional grain boundary scatterings should be considered for polycrystalline Ru. It seems that the resistivity of metals with a short λ, such as platinum-group metals, are insensitive to surface scatterings. Therefore, in order to further reduce the resistivity of metals with short λ values, such as Ru, Rh, and Ir, reducing grain boundary scatterings by increasing the grain size or improving the grain boundary is more effective than reducing the surface scattering.

As mentioned in the introduction, the deposition method is crucial for future metals like Ru, Rh and Ir to be adjusted to practical BEOL processes. ALD is a powerful tool to fill metal into shallow trenches conformally instead of using PVD, such as a sputtering or e-beam evaporator. Unlike Rh and Ir, ALD Ru has been developed with various precursors [44], [45], [46], [47]. Thus, we studied the resistivities of ALD-deposited metals based on Ru.

The resistivities of ALD Ru films are shown in Fig. 6(a) along with the calculated resistivity lines (red) of sputter Ru films based on the experimental results. The resistivity of ALD Ru lies between the as-deposited and annealed sputter Ru films at thicknesses of 10 nm or more. This is mainly due to the grain sizes of ALD Ru films at 220 °C, which are in between the sizes of the as-deposited

and annealed sputter films (not shown here). However, the resistivity of a ALD Ru film is rapidly increased in thickness regions thinner than 10 nm, which crossover with that of as-deposited sputter Ru at 8 nm. In order to investigate the origin of the resistivity of ALD Ru at the initial deposition stage, we analyzed the surface of Ru films. Fig. 6(b) shows the RMS roughness of Ru films deposited by both ALD and sputtering that depend on the thickness. As shown in Fig. 6(b), the sputter Ru films exhibit a similar RMS roughness of 0.3–0.5 nm regardless of the thickness and annealing so we do not need to consider the roughness effects on the resistivity. Conversely, ALD Ru films had rougher surfaces with a higher RMS roughness of 1.8 nm at the initial deposition stage (thickness of approximately 5 nm). As the thickness increases to 10 nm, the surfaces are rapidly smoothened with the decreased RMS roughness of 1 nm. We can observe that the smooth surfaces are maintained beyond the thickness of 10 nm. This phenomenon is due to the ALD process, including nucleation, lateral growth, and coalescence. From the results in which the roughness trend of ALD Ru is similar to its resistivity trend, we believe that the surface roughness is another factor to be considered in addition to electron scatterings at the grain boundaries and surfaces. To confirm the degree of resistivity increase because of the roughness, it was compared with the calculation result using (1), where the roughness effect is not considered. Despite the high surface RMS roughness of 1 nm, the calculated lines in the thick region are comparable and have an R value of 0.68. However, the difference between the experimental and calculation results rapidly increased when the thickness was decreased to below 10 nm, showing a large difference of 30 $\mu\Omega$-cm even if the surface is fully diffusive at a thickness of 6 nm. This proves that the increase in resistivity due to the rough surface effect should be considered in thin regions, i.e., less than 10 nm. According to the electron trajectories by the Monte Carlo model provided by Kuan et al., the random nature of the surface roughness reflects electrons irrespective of the direction of the electron field, causing a rapid increase in the resistivity [35].

V. CONCLUSION

We investigated the scaling effects of Ru, Rh, and Ir on their resistivities at thicknesses in the range 4–32 nm. Their resistivities were lower than that of Cu at thicknesses below 10 nm. Despite their similar electron mean free paths, their resistivities decreased in the order of Ru, Ir and Rh, following the order of their bulk resistivities at thicknesses below 10 nm. Although the bulk resistivity of Ir is lower than that of Ru, their resistivities became similar at thicknesses above 10 nm. TEM analyses confirmed that the high resistivity of Ir is due to its small grain size. This tendency was maintained after annealing at 400 °C. From the resistivity modeling done using the FS and MS models, we determined that while the effects of their surface scatterings are limited, grain boundary scatterings significantly influence the resistivities of Ru, Rh, and Ir. In addition, through the resistivity of ALD Ru, the effect of the surface roughness on the resistivity was also investigated. The high RMS surface roughness of approximately 2 nm at a thickness of 6 nm caused a considerable increase in the resistivity to 62 $\mu\Omega$-cm, which is far from the calculated resistivity. These results present multiple points for consideration when applying short mean free path metals to finite size interconnects.

REFERENCES

[1] C. K. Hu, R. Rosenberg, and K. Y. Lee, "Electromigration path in Cu thin-film lines," *Appl. Phys. Lett.*, vol. 74, pp. 2945–2947, May 1999, doi: 10.1063/1.123974.
[2] D. N. Bhate, A. Kumar, and A. F. Bower, "Diffuse interface model for electromigration and stress voiding," *J. Appl. Phys.*, vol. 87, pp. 1712–1721, Jan. 2000, doi: 10.1063/1.372082.
[3] D. Josell, S. H. Brongersma, and Z. Tokei, "Size-dependent resistivity in nanoscale interconnects," *Annu. Rev. Mater. Res.*, vol. 39, pp. 231–254, Aug. 2009, doi: 10.1146/annurev-matsci-082908-145415.
[4] T. Sun et al., "Dominant role of grain boundary scattering in the resistivity of nanometric Cu films," *Phys. Rev. B, Condens. Matter*, vol. 79, Jan. 2009, Art. no. 41402, doi: 10.1103/PhysRevB.79.041402.
[5] R. L. Graham et al., "Resistivity dominated by surface scattering in sub-50 nm Cu wires," *Appl. Phys. Lett.*, vol. 96, Jan. 2010, Art. no. 42116, doi: 10.1063/1.3292022.
[6] D. Gall, "Electron mean free path in elemental metals," *J. Appl. Phys.*, vol. 119, Feb. 2016, Art. no. 85101, doi: 10.1063/1.4942216.
[7] K. Fuchs, "The conductivity of thin metallic films according to the electron theory of metals," *Proc. Cambridge Philos. Soc.*, vol. 34, pp. 100–108, Jan. 1938, doi: 10.1017/S0305004100019952.
[8] E. H. Sondheimer, "The mean free path of electrons in metals," *Adv. Phys.*, vol. 50, pp. 499–537, Nov. 2010, doi: 10.1080/00018730110102187.
[9] A. F. Mayadas, M. Shatzkes, and J. F. Janak, "Electrical resistivity model for polycrystalline films: The case of specular reflection at external surfaces," *Appl. Phys. Lett.*, vol. 14, pp. 345–347, Jun. 1969, doi: 10.1063/1.1652680.
[10] A. F. Mayadas and M. Shatzkes, "Electrical-resistivity model for polycrystalline films: The case of arbitrary reflection at external surfaces," *Phys. Rev. B, Condens. Matter*, vol. 1, pp. 1382–1389, Feb. 1970, doi: 10.1103/PhysRevB.1.1382.
[11] K. H. Min, K.-C. Chun, and K.-B. Kim, "Comparative study of tantalum and tantalum nitrides (Ta_2N and TaN) as a diffusion barrier for Cu metallization," *J. Vac. Sci. Techol. B*, vol. 14, pp. 3263–3269, Sep. 1996, doi: 10.1116/1.588818.
[12] S. Q. Wang, I. Raaijmakers, B. J. Burrow, S. Suthar, S. Redkar, and K.-B. Kim, "Reactively sputtered TiN as a diffusion barrier between Cu and Si," *J. Appl. Phys.*, vol. 68, pp. 5176–5187, Nov. 1990, doi: 10.1063/1.347059.
[13] S. Dutta et al., "Thickness dependence of the resistivity of platinum-group metal thin films," *J. Appl. Phys.*, vol. 122, Art. no. 025107, Jul. 2017, doi: 10.1063/1.4992089.
[14] L. Jablonka, L. Riekehr, Z. Zhang, S. L. Zhang, and T. Kubart, "Highly conductive ultrathin Co films by high-power impulse magnetron sputtering," *Appl. Phys. Lett.*, vol. 112, Jan. 2018, Art. no. 43103, doi: 10.1063/1.5011109.
[15] M. Wislicenus, R. Liske, L. Gerlich, B. Vasilev, and A. Preusse, "Cobalt advanced barrier metallization: A resistivity composition analysis," *Microelectron. Eng.*, vol. 137, pp. 11–15, Apr. 2015, doi: 10.1016/j.mee.2014.09.017.
[16] L. G. Wen et al., "Atomic layer deposition of ruthenium with TiN interface for sub-10 nm advanced interconnects beyond copper," *ACS Appl. Mater. Interfaces*, vol. 8, pp. 26119–26125, Sep. 2016, doi: 10.1021/acsami.6b07181.
[17] E. Milosevic, S. Kerdsongpanya, A. Zangiabadi, K. Barmak, K. R. Coffey, and D. Gall, "Resistivity size effect in epitaxial Ru(0001) layers," *J. Appl. Phys.*, vol. 124, Oct. 2018, Art. no. 165105, doi: 10.1063/1.5046430.

[18] H. Y. Lee, Y. W. Hsieh, C. H. Hsu, and K. S. Liang, "Characteristics of sputter-deposited Ru thin films on Si substrates," *Mater. Chem. Phys.*, vol. 82, pp. 984–990, Dec. 2003, doi: 10.1016/j.matchemphys.2003.08.022.
[19] A. Jog and D. Gall, "Resistivity size effect in epitaxial iridium layers," *J. Phys. Lett.*, vol. 130, Sep. 2021, Art. no. 115103, doi: 10.1063/5.0060845.
[20] C. Perez et al., "Dominant energy carrier transitions and thermal anisotropy in epitaxial iridium thin films," *Adv. Funct. Mater.*, vol. 32, Aug. 2022, Art. no. 2207781, doi: 10.1002/adfm.202207781.
[21] K. Croes et al., "Interconnect metals beyond copper: Reliability challenges and opportunities," in *IEDM Tech. Dig.*, vol. 1, Dec. 2018, p. 5, doi: 10.1109/IEDM.2018.8614695.
[22] M. Popovici et al., "Atomic layer deposition of ruthenium thin films from (ethylbenzyl) (1-ethyl-1,4-cyclohexadienyl) Ru: Process characteristics, surface chemistry, and film properties," *Chem. Mater.*, vol. 29, pp. 4654–4666, May 2017, doi: 10.1021/acs.chemmater.6b05437.
[23] T. Aaltonen, P. Alen, M. Ritala, and M. Leskela, "Ruthenium thin films grown by atomic layer deposition," *Chem. Vap. Deposit.*, vol. 9, pp. 45–49, Jan. 2003, doi: 10.1002/cvde.200290007.
[24] S. S. Yim, D. J. Lee, K. S. Kim, S. H. Kim, T. S. Yoon, and K. B. Kim, "Nucleation kinetics of Ru on silicon oxide and silicon nitride surfaces deposited by atomic layer deposition," *J. Appl. Phys.*, vol. 103, Jun. 2008, Art. no. 113509, doi: 10.1063/1.2938052.
[25] S. K. Kim et al., "Atomic layer deposition of Ru thin films using 2,4-(dimethylpentadienyl)(ethylcyclopentadienyl)Ru by a liquid injection system," *J. Electrochem. Soc.*, vol. 154, p. D95, Jan. 2007, doi: 10.1149/1.2403081.
[26] E. F. McCullen, C. L. Hsu, and R. G. Tobin, "Electron density changes and the surface resistivity of thin metal films: Oxygen on Cu(100)," *Surf. Sci.*, vol. 481, pp. 198–204, Jun. 2001, doi: 10.1016/S0039-6028(01)01041-X.
[27] E. T. Krastev, D. E. Kuhl, and R. G. Tobin, "Multiple mechanisms for adsorbate-induced resistivity: Oxygen and formate on Cu(100)," *Surf. Sci.*, vol. 387, pp. L1051–L1056, Oct. 1997, doi: 10.1016/S0039-6028(97)00439-1.
[28] J. S. Chawla, F. Zahid, H. Guo, and D. Gall, "Effect of O_2 adsorption on electron scattering at Cu(001) surfaces," *Appl. Phys. Lett.*, vol. 97, Sep. 2010, Art. no. 132106, doi: 10.1063/1.3489357.
[29] D. Dayal and P. Wissmann, "The effect of gas adsorption on the electrical resistivity of thin gold films," *Vak.-Tech.*, vol. 38, nos. 5–6, pp. 121–133, 1989.
[30] E. Schmiedl, M. Watanabe, P. Wissmann, and E. Wittmann, "The effect of gas adsorption on the electrical resistivity of thin silver films," *Appl. Phys. A*, vol. 35, pp. 13–17, Sep. 1984, doi: 10.1007/BF00620294.
[31] J. M. Camacho and A. I. Oliva, "Surface and grain boundary contributions in the electrical resistivity of metallic nanofilms," *Thin Solid Films*, vol. 515, pp. 1881–1885, Dec. 2006, doi: 10.1016/j.tsf.2006.07.024.
[32] H. D. Liu, Y. P. Zhao, G. Ramanath, S. P. Murarka, and G. C. Wang, "Thickness dependent electrical resistivity of ultrathin (<40 nm) Cu films," *Thin Solid Films*, vol. 384, pp. 151–156, Mar. 2001, doi: 10.1016/S0040-6090(00)01818-6.
[33] J. S. Chawla, F. Gstrein, K. P. O'Brien, J. S. Clarke, and D. Gall, "Electron scattering at surfaces and grain boundaries in Cu thin films and wires," *Phys. Rev. B, Condens. Matter*, vol. 84, Dec. 2011, Art. no. 235423, doi: 10.1103/PhysRevB.84.235423.
[34] W. Zhang et al., "Influence of the electron mean free path on the resistivity of thin metal films," *Microelectron. Eng.*, vol. 76, pp. 146–152, Oct. 2004, doi: 10.1016/j.mee.2004.07.041.
[35] S. M. Rossnagel and T. S. Kuan, "Alteration of Cu conductivity in the size effect regime," *J. Vac. Sci. Technol. B*, vol. 22, pp. 240–247, Jan. 2004, doi: 10.1116/1.1642639.
[36] K. Sivaramakrishnan and T. L. Alford, "Metallic conductivity and the role of copper in ZnO/Cu/ZnO thin films for flexible electronics," *Appl. Phys. Lett.*, vol. 94, Feb. 2009, Art. no. 52104, doi: 10.1063/1.3077184.
[37] J. W. Lim, K. Mimura, and M. Isshiki, "Thickness dependence of resistivity for Cu films deposited by ion beam deposition," *Appl. Surf. Sci.*, vol. 217, pp. 95–99, Jul. 2003, doi: 10.1016/S0169-4332(03)00522-1.
[38] N. A. Lanzillo and D. C. Edelstein, "Reliability and resistance projections for rhodium and iridium interconnects from first-principles," *J. Vac. Sci. Technol. B*, vol. 40, Aug. 2022, Art. no. 52801, doi: 10.1116/6.0001980.
[39] R. D. Doherty et al., "Current issues in recrystallization: A review," *Mater. Sci. Eng. A*, vol. 238, pp. 219–274, Nov. 1997, doi: 10.1016/S0921-5093(97)00424-3.
[40] T. H. Kim et al., "Structural dependence of grain boundary resistivity in copper nanowires," *Jpn. J. Appl. Phys.*, vol. 50, Aug. 2011, Art. no. 8LB09, doi: 10.1143/JJAP.50.08LB09.
[41] T. H. Kim et al., "Large discrete resistance jump at grain boundary in copper nanowire," *Nano Lett.*, vol. 10, pp. 3096–3100, Jul. 2010, doi: 10.1021/nl101734h.
[42] D. Gall, "The search for the most conductive metal for narrow interconnect lines," *J. Appl. Phys.*, vol. 127, Feb. 2020, Art. no. 50901, doi: 10.1063/1.5133671.
[43] S. S. Ezzat et al., "Resistivity and surface scattering of (0001) single crystal ruthenium thin films," *J. Vac. Sci. Technol. A*, vol. 37, May 2019, Art. no. 31516, doi: 10.1116/1.5093494.
[44] T. K. Eom et al., "Low temperature atomic layer deposition of ruthenium thin films using isopropylmethylbenzene-cyclohexadiene-ruthenium and O_2," *Electrochem. Solid-State Lett.*, vol. 12, p. D85, Aug. 2009, doi: 10.1149/1.3207867.
[45] O. K. Kwon, S. H. Kwon, H. S. Park, and S. W. Kang, "Plasma-enhanced atomic layer deposition of ruthenium thin films," *Electrochem. Solid-State Lett.*, vol. 7, p. C46, Feb. 2004, doi: 10.1149/1.1648612.
[46] K. Kukli et al., "Atomic layer deposition of ruthenium films from (ethylcyclopentadienyl)(pyrrolyl)ruthenium and oxygen," *J. Electrochem. Soc.* vol. 158, p. D158, Jan. 2011, doi: 10.1149/1.3533387.
[47] D. S. Kwon et al., "Atomic layer deposition of Ru thin films using (2,4-dimethyloxopentadienyl)(ethylcyclopentadienyl)Ru and the effect of ammonia treatment during the deposition," *J. Mater. Chem. C*, vol. 8, pp. 6993–7004, Apr. 2020, doi: 10.1039/D0TC01489C.